

67, 235 (1995)], the details of which are described in (5). During this study, total chemistry and mass spectrometry blanks were 6 pg for Re and 2 pg for Os, with a $^{187}\text{Os}/^{188}\text{Os}$ blank ratio of 0.175. Blank corrections were insignificant for all samples analyzed in this study. Over a 3-year period, repeated analyses of an Os isotopic mass spectrometry standard provided by the Carnegie Institution of Washington, Department of Terrestrial Magnetism (DTM), made with Johnson-Matthey ammonium hexachlorosmate batch 5.56870-A, yielded mean $^{187}\text{Os}/^{188}\text{Os} = 0.17367 \pm 0.00058$ [external reproducibility at the 2σ level ($n = 24$) using a peak-jumping routine and a secondary electron multiplier], within error of the DTM value of 0.17429 ± 0.00055 [S. B. Shirey, *Can. J. Earth Sci.* **34**, 489 (1997)] (5). There is no measurable bias introduced into the data from our mass spectrometer (Finnigan MAT 262 N-TIMS) relative to results produced at DTM.

20. R. J. Walker, R. W. Carlson, S. B. Shirey, F. R. Boyd, *Geochim. Cosmochim. Acta*, **53**, 1583 (1989); M. Roy-Barman and C. J. Allegre, *ibid.* **58**, 5043 (1994); J. E. Snow and L. Reisberg, *Earth Planet. Sci. Lett.* **133**, 411 (1995).

21. The Lihir ore samples are from the Ladolam gold deposit and were selected from G. Carman's (1993) unpublished Ph.D. thesis collection, Monash University. Sample 101373 is a biotite-altered basaltic breccia from the Minifie area containing the following alteration assemblage: biotite, potassium-containing feldspar (k-feldspar), anhydrite, calcite, pyrite, albite, quartz, adularia, chalcophyrite, tetrahedrite, electrum, galena, sphalerite, and argentite. Sample 101201 is a heterolithic breccia of mainly mafic lavas from the Lienetz area containing the following alteration assemblage: biotite, tourmaline, k-feldspar, albite, sericite, pyrite, magnetite, anhydrite, calcite, marcasite, and pyrrhotite.

22. K-Ar ages reported for various stages of hydrothermal alteration at the Ladolam gold deposit on Lihir island include the following: biotite separate from potassic altered volcanic rock age of 917 ± 100 Ka, biotite separate from biotite pyroxenite monzonite age of 343 ± 36 Ka, biotite separate from biotite-anhydrite vein age of 336 ± 27 Ka, and alunite-rich whole rock age of 151 ± 15 Ka [R. M. Davies and G. H. Ballantyne, in *PACRIM Congress 1987* (Australasian Institute of Mining and Metallurgy, Gold Coast, Australia, 1987), vol. 1, pp. 943-994].

23. CO_2 for oxygen isotope analysis was prepared as described by Clayton and Mayeda [R. N. Clayton and T. K. Mayeda, *Geochim. Cosmochim. Acta* **27**, 43 (1963)]. Samples were finely ground and heated in Ni reaction vessels with BrF_3 at 650°C for 14 hours. The CO_2 was analyzed automatically on a Finnigan 252 mass spectrometer against an internal standard. Two quartz standards were run with every 10 samples. Replicate analysis of the standard quartz is generally better than ± 0.2 . Analyses are reported in per mil relative to the standard mean ocean water (SMOW) standard.

24. D. E. James, *Annu. Rev. Earth. Planet. Sci.* **9**, 311 (1981).

25. T. K. Kyser, in *Stable Isotopes in High Temperature Geological Processes*, J. W. Valley, H. P. Taylor Jr., J. R. O'Neill, Eds. (Mineralogical Society of America, Washington, DC, 1986), vol. 16, pp. 141-164.

26. J. D. Cocker, B. J. Griffin, K. Muehlenbachs, *Earth Planet. Sci. Lett.* **61**, 112 (1982); R. T. Gregory and H. P. Taylor Jr., *J. Geophys. Res.* **86**, 2737 (1981); K. Muehlenbachs, in *Stable Isotopes in High Temperature Geological Processes*, J. W. Valley, H. P. Taylor Jr., J. R. O'Neill, Eds. (Mineralogical Society of America, Washington, DC, 1986), vol. 16, pp. 425-444.

27. Melt inclusions from mantle wedge samples from the Tabar-Lihir-Tanga-Feni island arc are enriched in ^{18}O , with $\delta^{18}\text{O}$ values ranging from 9.0 to $11.3\text{‰} \pm 1.1\text{‰}$; J. M. Eiler, B. I. A. McInnes, J. W. Valley, C. M. Graham, E. M. Stolper, *Nature* **393**, 777 (1998).

28. The calculations follow the method outlined in (6). The Os abundances in the oceanic basalt and oceanic sediment were assumed to be equal. The Os isotopic composition of the subduction component was calculated with the following parameters: oceanic sediment $^{187}\text{Os}/^{188}\text{Os} = 1.023$ [an average value based on references in (6)] and oceanic basalt $^{187}\text{Os}/$

$^{188}\text{Os} = 2.117$ (assumes slab basalt has $^{187}\text{Os}/^{188}\text{Os}$ equivalent to gabbro sample 136033 in Table 1). Therefore, a 95% slab basalt containing 5% oceanic sediment slab component will have $^{187}\text{Os}/^{188}\text{Os} = 2.062$. The depleted peridotite end-member component was assumed to have an isotopic composition equivalent to harzburgite sample 136063 in Table 1 ($^{187}\text{Os}/^{188}\text{Os} = 0.1217$ and $\delta^{18}\text{O} = 4.9\text{‰}$). The $\delta^{18}\text{O}$ for the subduction component is ascribed a value of 12‰ based on $\delta^{18}\text{O}$ measurements of subduction-derived metasomatic agents with $\delta^{18}\text{O} = 11.3\text{‰}$ from mantle wedge xenocrysts found elsewhere in the Tabar-Lihir-Tanga-Feni arc (27). The value of 12‰ is consistent with values obtained from seawater-altered basalt (5.7 to 12‰) from the upper 1 to 2 km of oceanic crust from ophiolite sequences (26).

29. Modeling assumes simple bulk mixing between Lihir

melt ($^{187}\text{Os}/^{188}\text{Os} = 0.167$, Os = 0.080 ppb; sample 136000 in Table 1) and peridotite mantle [$^{187}\text{Os}/^{188}\text{Os} = 0.122$ to 0.1271, Os = 3.5 ppb; see Table 1 and (8)].

30. S. B. Shirey and R. W. Walker, *Anal. Chem.* **67**, 2136 (1995).

31. R. H. Mitchell and R. R. Keays, *Geochim. Cosmochim. Acta* **45**, 2425 (1981).

32. S. R. Hart and G. Ravizza, *Eos* **120** (1993).

33. W. F. McDonough and S.-s. Sun, *Chem. Geol.* **120**, 223 (1995).

34. We thank John Byrne and Jim Keegan for assistance in determining PGE contents, Brad McDonald for oxygen isotope analysis, and Eva Mylka for drafting. The comments of the anonymous reviewers helped clarify the presentation.

22 June 1999; accepted 3 September 1999

Continuous Deformation Versus Faulting Through the Continental Lithosphere of New Zealand

Peter Molnar,^{1*} Helen J. Anderson,^{2,3,4} Etienne Audoin,⁵ Donna Eberhart-Phillips,³ Ken R. Gledhill,⁶ Eryn R. Klosko,^{7,8} Thomas V. McEvilly,⁹ David Okaya,¹⁰ Martha Kane Savage,⁵ Tim Stern,⁵ Francis T. Wu⁷

Seismic anisotropy and *P*-wave delays in New Zealand imply widespread deformation in the underlying mantle, not slip on a narrow fault zone, which is characteristic of plate boundaries in oceanic regions. Large magnitudes of shear-wave splitting and orientations of fast polarization parallel to the Alpine fault show that pervasive simple shear of the mantle lithosphere has accommodated the cumulative strike-slip plate motion. Variations in *P*-wave residuals across the Southern Alps rule out underthrusting of one slab of mantle lithosphere beneath another but permit continuous deformation of lithosphere shortened by about 100 kilometers since 6 to 7 million years ago.

In most oceanic regions, plates of lithosphere move past one another along narrow boundaries (width <20 km), and a single major fault can

define transform and convergent boundaries; active deformation within continental regions, however, commonly spans dimensions of hundreds to thousands of kilometers. The much greater creep strength of olivine than of crustal minerals makes oceanic lithosphere strong in the depth range where continental lithosphere appears to be weakest (*J*). What then is the role of the mantle lithosphere beneath continents? Is it cut by faults, or narrow shear zones, that separate effectively rigid bodies, as if plate tectonics occurred but was blurred by the easily deformed overlying crust (2, 3); or does the mantle lithosphere deform continuously over a wide area, behaving as a continuous medium (4, 5) (Fig. 1)? New Zealand offers tests of these possibilities. Since ~45 million years ago (Ma), the Pacific and Australian plates have slid 850 (± 100) km past one another, with ~460 km of right-lateral slip on a single major fault, the Alpine fault, dominating Cenozoic deformation of New Zealand's crust (6, 7). Does the Alpine fault cut through the entire lithosphere, or does widespread simple shear

¹Quaternary Research Center and Geophysics Program, University of Washington, Seattle, WA, 98195-1360, USA, and Department of Earth Atmospheric and Planetary Sciences, Massachusetts Institute of Technology, Cambridge, Massachusetts 02139, USA. ²Ministry of Research, Science and Technology, Post Office Box 5336, Wellington, New Zealand. ³Institute of Geological and Nuclear Sciences, Private Bag 1930, Dunedin, New Zealand. ⁴Otago University, Dunedin, New Zealand. ⁵Institute of Geophysics, School of Earth Sciences, Victoria University of Wellington, Wellington, New Zealand. ⁶Institute of Geological and Nuclear Sciences, Gracefield Research Centre, Post Office Box 30-368 Lower Hutt, Wellington, New Zealand. ⁷Department of Geological Sciences, State University of New York, Binghamton, NY, 13902, USA. ⁸Department of Geological Sciences, 1847 Sheridan Road, Lucy Hall, Northwestern University, Evanston, IL 60208, USA. ⁹Berkeley Seismological Laboratory, University of California, Berkeley, CA 94720, USA. ¹⁰Department of Earth Sciences, University of Southern California, Los Angeles, CA 90089, USA.

*To whom correspondence should be addressed. E-mail: molnar@chandler.mit.edu

parallel to the fault occur throughout the underlying mantle lithosphere? At ~6 to 7 Ma, the direction of relative movement between the Pacific and Australian plates changed somewhat, resulting in ~100 km of convergence across the South Island of New Zealand (8). Has "intracontinental subduction" of mantle lithosphere occurred (2, 9), or has mantle lithosphere deformed continuously (4, 5)? We compare magnitudes of relative plate motion across the Pacific-Australian plate boundary in New Zealand with estimates of strain in the underlying mantle from recent seismological studies to address these questions (10, 11).

After a period of Mesozoic subduction, Cenozoic deformation began in Late Eocene or Early Oligocene time, at ~35 to 45 Ma (12) and has distorted that ancient subduction boundary. On the North Island, a prominent magnetic anomaly, the Junction Magnetic Anomaly (13), follows that subduction zone through the Dun Mountain ophiolite belt, is offset by the Alpine fault, and then continues across the South Island (Fig. 2). The 45-Ma reconstruction of New Zealand aligns the straight segments of the Junction Magnetic Anomaly, implying that simple shear in a zone ~100 to 150 km wide has bent the geologic belts southeast of the Alpine fault and absorbed ~150 km of right-lateral displacement (7, 14). Similarly, its curved continuation into the North Island implies considerable right-lateral shear of it, perhaps as much as 250 km over a zone 250 to 300 km wide in its northwest-southeast dimension. Paleomagnetic declinations of Oligocene sediment (~35 Ma) close to the Junction Magnetic Anomaly indicate essentially no

rotation of the northwestern part of the North Island with respect to Australia (Fig. 2); ~30° of clockwise rotation in the central North Island, as might be expected from the curvature of the Junction Magnetic Anomaly; and almost 80° near Dun Mountain (15). Thus, of ~850 km of right-lateral displacement between the Pacific and Australian plates in the New Zealand area, ~400 km seem to have been accommodated by distributed right-lateral simple shear of the crust across a zone ~400 km wide (Fig. 2). Currently, right-lateral slip on the Alpine fault accounts for about two-thirds of the strike-slip component of plate motion as seen at the surface (16, 17). Such rates imply that localization of crustal strain on that fault began before 6 to 7 Ma.

The change in relative motion at 6 to 7 Ma (8) apparently marked the birth of the Southern Alps. Accelerated cooling of rock beginning at ~7 Ma (18) and rapid sedimentation on the west coast beginning ~5 Ma (19) surely reflect increased erosion associated with crustal shortening and thickening. The initiation of slip on at least some of the Marlborough strike-slip faults (20) also presumably resulted from a redistribution of deformation. Although a reverse component of slip on the Alpine fault has absorbed a substantial fraction of the convergence between the Pacific and Australian plates (21), both active faulting and current deformation revealed by GPS measurements demonstrate ongoing crustal straining of the entire island (17).

Finite strain of the mantle reveals itself by anisotropic seismic wave propagation, demonstrated most clearly by the splitting of shear waves into two orthogonally polarized quasi-S waves (22). A preferred alignment of intrinsi-

cally anisotropic crystals causes anisotropy in the mantle, where pressure is too high for cracks to remain open (23). Both observations (23) and calculations based on simple theory for large finite strain (24) show the maximum difference in S-wave speeds when propagation is parallel to the intermediate principal axis of strain. Propagation is fastest for waves polarized parallel to the axis of maximum extension and slowest for waves polarized parallel to the axis of maximum flattening. Thus, S waves propagating steeply through an anisotropic layer should be split most where large strike-slip strain has occurred in that layer. For sufficiently large strain, the quasi-S wave polarized parallel to the plane of shear propagates faster than those perpendicular to it (24).

Shear-wave splitting at most stations on New Zealand (10, 25) shows that polarizations of the faster S waves are oriented nearly parallel to the strike of the Alpine fault, with magnitudes of splitting exceeding 1 s at nearly all stations and reaching 2 s at several (Fig. 3). Measurements at stations on the Chatham and Macquarie Islands, ~1000 km from the rest, show different patterns (inset, Fig. 3), consistent with anisotropy beneath New Zealand being due to deformation of New Zealand lithosphere and not to shear along its base as it moves over the asthenosphere. Fast polarizations at stations in the southern part of the South Island, where strike-slip strain should be least, are oriented up to 30° from the fault. At most stations across the Southern Alps and northwest of the Alps and at station WLZA on the North Island, which include those with the largest magnitudes of splitting, orientations of fast polarizations lie within 10° of the Alpine fault.

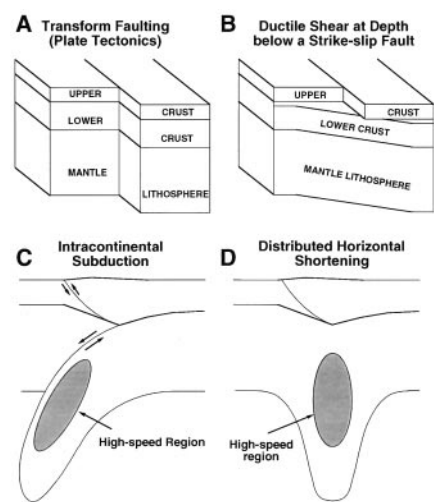
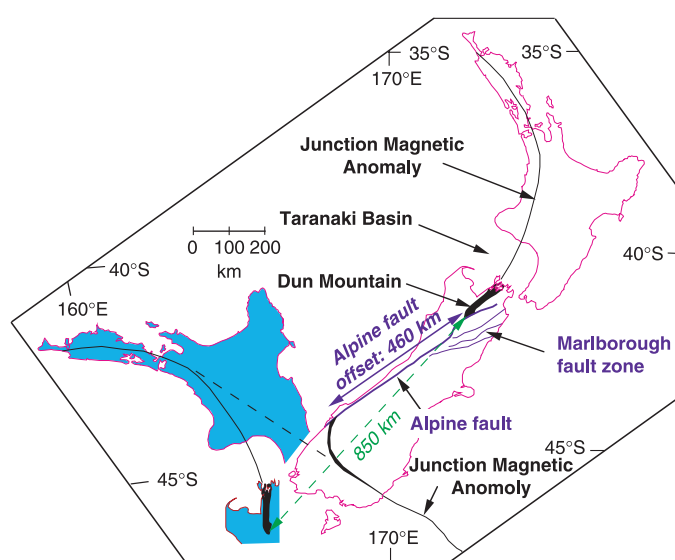


Fig. 1. Cartoons illustrating two extreme views of deformation of mantle lithosphere for strike-slip (A and B) and convergent (C and D) relative movement. Fault zones penetrating both crust and upper mantle, as for plate tectonics, are shown on the left [(A) and (C)], and a simple image of continuous deformation of the mantle lithosphere is shown on the right [(B) and (D)].

Fig. 2. Simplified map of present geology (white area in red outline) and a reconstruction appropriate for 45 Ma (blue area in red outline). The important geologic feature shown here is the belt of ultramafic rock, the Maitai terrane, whose continuation north of the Alpine fault passes through Dun Mountain, of dunite fame (7). This belt can be traced beneath younger sediment using the Junction Magnetic Anomaly of Hatherton (13). Disruption of this belt by the Alpine fault implies ~460 km of displacement. The reconstructed position (6, 7) of the area north of the Alpine fault at ~45 Ma shows Dun mountain to have lain ~850 km southwest of its present position and not adjacent to the Maitai terrane across the Alpine fault. Presumably, the ultramafic belt and the Junction Magnetic Anomaly were once aligned across what is now the southwest end of the Alpine fault. Thus, ~390 km of plate motion must have been absorbed by slip on other, necessarily minor, faults or by more continuous penetrative strain [figure modified from Sutherland (7)].



REPORTS

We assume that anisotropy is concentrated in the lithosphere. Widespread extension and thinning in early Cenozoic time (12), followed by cooling of the plate, suggest a thickness of ~100 km (26). Flexure of New Zealand lithosphere beneath the Taranaki Basin (Fig. 2) suggests a value of ~25 km for the thickness of an equivalent elastic plate (27), also consistent with a lithospheric thickness of ~100 km (26). With a subjacent thermal boundary layer, we consider thicknesses of 125 and 250 km to allow for lithospheric thickening since 6 to 7

Ma. Shear-wave splitting of 2 s implies average fractional differences of $\delta v_s/v_s \sim 7\%$ and $\delta v_s/v_s \sim 4\%$ between maximum and minimum shear-wave speeds for propagation in the vertical direction through such thicknesses (δv_s is the difference between maximum and minimum quasi-S wave speeds, and v_s is the average speed).

Two processes can align anisotropic minerals: rotation of crystals in a finite strain field and dynamic recrystallization. Alone, rotation of randomly oriented olivine crystals, which in-

cludes internal deformation along their weakest planes, can create anisotropy as large as $\delta v_s/v_s = 4$ to 7% with only modest finite extensional strain of $\epsilon_{11} = 1.2$ to 1.5 (20 to 50% elongation) (24), a result confirmed by laboratory experiments (28). Calculations with a mixture of 70% olivine and 30% enstatite require at least $\epsilon_{11} = 1.5$ for $\delta v_s/v_s = 4\%$, and $\epsilon_{11} > 2$ for $\delta v_s/v_s = 7\%$ (24). With increasing strain, $\delta v_s/v_s$ approaches a maximum of 10%, with calculated orientations of fast polarizations parallel to the axis of maximum extension.

In a zone of width W undergoing simple shear by displacement d of the margins, $\epsilon_{11} = \cot \theta$ (with maximum flattening strain $\epsilon_{33} = \tan \theta$), where θ is the angle between the axis of maximum extension and the shear zone, and $\tan 2\theta = 2W/d$. Even for 100% extension ($\epsilon_{11} = 2$), $\theta = 27^\circ$, and for $\epsilon_{11} = 1.5$, $\theta = 34^\circ$. If no other process caused a preferred orientation of the crystals, extension of $\epsilon_{11} \approx 6$ would be needed to rotate fast axes within 10° of the shear zone. Zhang and Karato (28), however, found in simple shear of olivine at high temperature (1300°C) and strain rate (10^{-5} s^{-1}), when $d/W = 1.5$ ($\epsilon_{11} = 2$), enough recrystallization had occurred that fast axes became nearly parallel to the plane of shear. At 1200°C, dynamic recrystallization was much smaller; but presumably at lower strain rates, dynamic recrystallization would be important at lower temperatures, if temperatures might be too low in the shallowest mantle for significant recrystallization. Clearly, making accurate inferences of strain from measurements of shear-wave splitting remains impossible, but it appears that large magnitudes of splitting ($\delta v_s/v_s \geq 4\%$) with the orientations of fast S-wave polarizations nearly parallel to the plane of simple shear imply shear strain corresponding to $d/W > 1.5$ and perhaps much larger.

The nearly parallel orientations of fast polarization at sites 100 to 150 km southeast of the Alpine fault and at comparable distances northwest of its projection into both the northern South Island and the North Island (Fig. 3) indicate that strain has occurred over a zone at least as wide as 300 km. Shortening of ~100 km across the island since 6 to 7 Ma suggests that strike-slip shear strain occurred over a zone ~400 km wide. If the magnitudes of splitting imply strains corresponding to $d/W = 1.5$, then with $W = 400 \text{ km}$, $d = 600 \text{ km}$, which exceeds the offset on the Alpine fault and is more than two-thirds of the 850-km cumulative right-lateral plate motion across New Zealand (6, 7). Given that $d/W = 1.5$ is a lower bound, the shear-wave splitting is consistent with all plate motion being absorbed in the lithosphere by distributed strain, and it permits only a small fraction of that motion to occur by strike-slip faulting in the mantle.

In this discussion, we have ignored the strain due to horizontal shortening of the lithosphere, in part because that strain is smaller

Fig. 3. Map of New Zealand showing seismograph stations, measurements of shear-wave splitting (10, 25), locations of lines of seismographs used to determine the crustal structure (30) and upper mantle structure (11), and (hatched area) position of high-speed body in the depth range of 100 to 120 km (11). Lines through stations show the orientations of quasi-S waves with the faster polarization, and lengths of lines indicate the magnitude of splitting in seconds. Inset shows New Zealand and surrounding area with splitting results from the Chatham and Macquarie Islands. Lines with triangles show subduction zones with triangles pointing down dip.

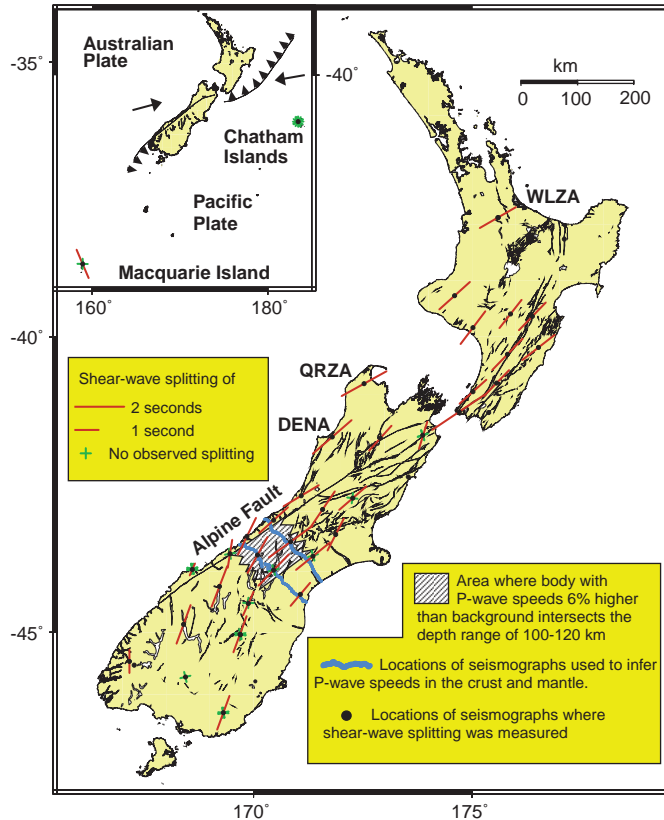
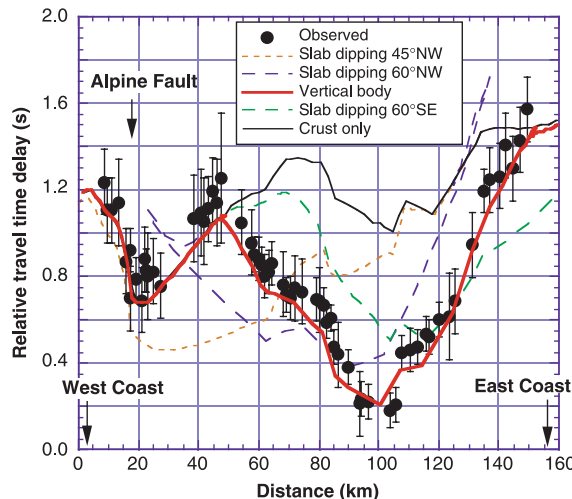


Fig. 4. P-Wave delays for propagation through hypothetical mantle structures beneath New Zealand. Plots of measured relative travel time delays (black points with error bars), and those calculated for the known crustal structure (30) and various mantle structures: crustal structure only (thin black line), a symmetric high-speed body beneath the region of thickest crust (dark red line), a slab of lithosphere dipping 45° northwest (dashed orange line), a slab of lithosphere dipping 60° northwest (dashed purple line), and a slab of lithosphere dipping 60° southeast (dashed green line). No significance should be attached to the magnitude of residuals; phases were correlated, instead of measuring first arrivals. Calculated delays are matched to observed delays at distances between 0 and 20 km. This earthquake occurred beneath Honshu, Japan, on 14 February 1996 at 21:26 56.4 GMT; 29.28°N, 140.45°E; depth = 141 km.



REPORTS

than the strike-slip shear and in part because pure flattening deformation induces smaller anisotropy than simple shear (24). Moreover, some of the largest splitting was measured at stations DENA and QRZA (Fig. 3) (10), where strike slip across the Marlborough faults absorbs most of the convergent component, and at WLZA, where subduction of the Pacific plate accommodates all convergence. Shortening could also contribute to the magnitude of splitting by increasing the thickness of the anisotropic layer, but again the large magnitudes of splitting at these stations argue against this contribution. Even if the convergent component enhanced the observed splitting, the conclusions that strain is widespread and that faulting must absorb at most a small fraction of plate motion would be unaltered. Only if large anisotropy could develop with small strains ($\epsilon_{11} < 1.5$) throughout the lithosphere and parallel to the sense of shear, or by strain throughout much of the underlying asthenosphere, could strike slip on a single fault zone account for more than half of the relative plate motion in New Zealand.

Shear-wave splitting at stations on the southeast side of the North Island (25), with fast polarizations parallel to those elsewhere in New Zealand (Fig. 3), might seem to require a common explanation for all anisotropy beneath New Zealand. Yet, *S* waves to stations on the southeast side of the North Island pass through Pacific lithosphere that has been underthrust beneath the North Island, not through mantle lithosphere attached to the deformed crust of New Zealand. Studies of the region east of the Tonga-Kermadec arc northeast of New Zealand using both seismic refraction and surface waves (29) reveal marked anisotropy within the Pacific plate, which suggests that the anisotropy in the lithosphere beneath the eastern North Island may have formed long before it was subducted. Moreover, large shear-wave splitting with fast orientations parallel to adjacent deep-sea trenches has been observed at stations above downgoing slabs in other island arcs, though this pattern is not common to all arcs (22). Thus, the shear-wave splitting measurements from the South Island and western North Island imply that the 850-km, right-lateral component of plate motion has been absorbed largely, if not entirely, by distributed simple shear in the mantle.

P-wave delays recorded by lines of seismographs across the Southern Alps (11) differ by up to 1 s from those expected for propagation through the laterally varying crustal structure (30) (Fig. 4) and therefore require marked lateral variation in the upper mantle. Elsewhere (11, 31) we present tests, using these delays, of whether one slab of mantle lithosphere underthrusts another on a single fault (2, 9) or deformation occurs by pure shear (horizontal shortening and thickening) across a zone of finite width. Because of the relatively thin lithosphere beneath New Zealand, the small amount of

convergence, ~ 100 km, should have perturbed structure only in the outer 200 km of the earth. At any depth, *P*-wave speeds will differ most where lateral temperature differences are largest and where the background temperature is near the solidus (32). Thus, we expect the largest anomaly in *P*-wave speeds to lie at a depth of ~ 100 to 120 km.

Stations with maximum *P*-wave advances from earthquakes to the northwest lie ~ 100 km southeast of the west coast (Fig. 4). The corresponding waves passed through the depth range of 100 to 120 km beneath the southeast flank of the Southern Alps (Fig. 3), where crust has thickened most (30, 33). Lithospheric thickening by pure shear would produce a high-speed zone in the upper mantle beneath the thickest crust. Northwestward underthrusting of a slab of Pacific mantle lithosphere (9), however, would place a high-speed zone at a depth of 100 to 120 km beneath the west coast and would advance *P*-wave arrivals from earthquakes to the northwest at stations on the western side of the island (Figs. 1C and 4). A slab of Australian lithosphere underthrust southeast (34) would put the high-speed zone too far to the southeast to account for the advances (Fig. 4). The *P*-wave residuals cannot rule out a slab of lithosphere that is sharply bent and plunging beneath the thickest crust, but such a geometry requires more strain than continuous deformation throughout the mantle lithosphere (11). Thus, both seismic anisotropy, which measures in situ strain, and *P*-wave residuals, which constrain the amount and distribution of lateral heterogeneity, suggest that the mantle lithosphere beneath continents deforms continuously and not by localized deformation on one or a small number of faults.

References and Notes

1. W. F. Brace and D. L. Kohlstedt, *J. Geophys. Res.* **85**, 6248 (1980).
2. M. Mattauer [*Geol. Soc. London Spec. Pub. No. 19* (1986), p. 37] coined the term "intracontinental subduction."
3. J.-P. Avouac and P. Tapponnier, *Geophys. Res. Lett.* **20**, 895, (1993); Ph. Matte et al., *Earth Planet. Sci. Lett.* **142**, 311 (1996); B. Meyer et al., *Geophys. J. Int.* **135**, 1 (1998).
4. R. I. Walcott, *Geophys. J. R. Astron. Soc.* **79**, 613 (1984).
5. S. Bourne, P. England, B. Parsons, *Nature* **391**, 655 (1998); P. England and G. Houseman, *J. Geophys. Res.* **91**, 3664 (1986); P. Molnar, in *Fault Mechanics and Transport Properties in Rocks: A Festschrift in Honor of W. F. Brace*, B. Evans and T.-f. Wong, Eds. (Academic Press, London, 1992), p. 435.
6. R. Sutherland, *Tectonics* **14**, 819 (1995).
7. ———, *N. Z. J. Geol. Geophys.* **42**, 295 (1999).
8. R. I. Walcott, *Rev. Geophys.* **36**, 1 (1998).
9. H. W. Wellman [*Bull. R. Soc. N. Z.* **18**, 13 (1979)] first proposed this mechanism, in particular for New Zealand. See also C. Beaumont, P. J. J. Kamp, J. Hamilton, P. Fullsack, *J. Geophys. Res.* **101**, 3333 (1996); J. Braun and C. Beaumont, *ibid.* **100**, 18059 (1995).
10. E. R. Klosko et al., *Geophys. Res. Lett.* **26**, 1497 (1999).
11. T. Stern, P. Molnar, D. Okaya, D. Eberhart-Phillips, in preparation.
12. R. M. Carter and R. J. Norris, *Earth Planet. Sci. Lett.* **31**, 85 (1976).

13. T. Hatherton N. Z. J. *Geol. Geophys.* **10**, 1330 (1967); *Geol. Soc. Am. Bull.* **80**, 213 (1969); R. Sutherland, *Tectonophysics* **308**, 341 (1999).
14. R. J. Norris, *Bull. R. Soc. N. Z.* **18**, 21 (1979).
15. T. C. Mumme and R. I. Walcott, *Paleomagnetic Studies at the Geophysics Division 1980–1983* (Report 204, Geophysics Division, Department of Scientific and Industrial Research, Wellington, New Zealand, 1985).
16. R. Sutherland and R. J. Norris, *N. Z. J. Geol. Geophys.* **38**, 419 (1995).
17. J. Beavan et al., *J. Geophys. Res.* in press.
18. J. M. Tippet and P. J. J. Kamp, *J. Geophys. Res.* **98**, 16119 (1993).
19. R. Sutherland, *N. Z. J. Geol. Geophys.* **39**, 251 (1996).
20. T. A. Little and A. Jones, *Tectonics* **17**, 285 (1998).
21. R. J. Norris, P. O. Koons, A. F. Cooper, *J. Struct. Geol.* **12**, 715 (1990); R. H. Sibson, S. H. White, B. K. Atkinson, *Bull. R. Soc. N. Z.* **18**, 55 (1979).
22. M. K. Savage *Rev. Geophys.* **27**, 64 (1999); P. G. Silver, *Annu. Rev. Earth Planet. Sci.* **24**, 385 (1996). Shear-wave splitting is the seismological analog of optical birefringence. A shear wave with arbitrary polarization from a distant earthquake and approaching the surface through an anisotropic layer will split into two orthogonally polarized quasi-shear waves that propagate with slightly different speeds. In the earth, the faster of these typically will arrive before the slower by 1 s or less, but in rare cases by 2 s (or more). The difference in arrival times depends on both the degree to which the material is anisotropic to propagation in the vertical direction and the thickness of anisotropic layer.
23. W. B. Ismail and D. Mainprice, *Tectonophysics* **296**, 145 (1998); D. Mainprice and P. G. Silver, *Phys. Earth Planet. Int.* **78**, 257 (1993); A. Nicolas and N. I. Christensen, in *Composition, Structure and Dynamics of the Lithosphere-Asthenosphere System*, *Geodynamics Series Vol. 16*, K. Fuchs and C. Froidevaux, Eds. (American Geophysical Union, Washington, DC, (1987), p. 111.
24. N. M. Ribe, *J. Geophys. Res.* **97**, 8737 (1992).
25. K. Marson-Pidgeon and M. K. Savage, *Geophys. Res. Lett.* **24**, 3297 (1997); K. Marson-Pidgeon, M. K. Savage, K. Gledhill, G. Stuart, *J. Geophys. Res.* **104**, 20277 (1999).
26. E. B. Burov and M. Diament, *J. Geophys. Res.* **100**, 3905 (1995).
27. W. E. Holt and T. A. Stern, *Earth Planet. Sci. Lett.* **107**, 523 (1991).
28. S. Zhang and Sh.-I. Karato, *Nature* **375**, 774 (1995).
29. P. M. Shearer and J. A. Orcutt, *Geophys. J. R. Astron. Soc.* **87**, 967 (1986); Y. Yu and J. Park, *J. Geophys. Res.* **99**, 15399 (1994).
30. A comprehensive experiment provides an unusually precise determination of the crustal structure [W. S. Holbrook et al., *Eos* **79** (suppl.), F901 (1998); M. Scherwath et al., *ibid.*, p. F901; T. A. Stern et al., *ibid.* **78**, 329 (1997)].
31. Stern et al. (11) reported *P*-wave residuals from three earthquakes lying northwest of New Zealand and recorded by a subset of stations along two lines across New Zealand (Fig. 3), used to determine the crustal structure (30). They present details of the analysis summarized here.
32. C. Goetze, in *High-Pressure Research, Applications to Geophysics*, M. H. Manghni and S.-I. Akimoto, Eds. (Academic Press, New York, 1977), p. 3; Sh.-I. Karato, *Geophys. Res. Lett.* **20**, 1623 (1993).
33. D. J. Woodward, *Bull. R. Soc. N. Z.* **18**, 95 (1979).
34. R. G. Allis, *Geology* **9**, 303 (1981); *Tectonics* **5**, 15 (1986).
35. We thank F. Davey, N. Godfrey, S. Henry, W. S. Holbrook, S. Kleffmann, A. Melhuish, M. Scherwath, and H. van Avendonk for sharing their images of the crustal structure of the South Island in advance of publication; N. I. Christensen for guidance with anisotropy; R. I. Walcott for insights; P. England and an anonymous referee for suggestions for improving the manuscript; and J. McRaney and the Incorporated Research Institutions in Seismology for logistical assistance of many kinds. Supported in part by the Continental Dynamics Program of NSF (grant EAR-9418530), the New Zealand Public Good Science Fund, and the Marsden Research Fund in New Zealand.

3 June 1999; accepted 8 September 1999